



Available online at <http://scik.org>

J. Math. Comput. Sci. 11 (2021), No. 5, 5682-5702

<https://doi.org/10.28919/jmcs/6098>

ISSN: 1927-5307

FINITE ELEMENT SOLUTION OF MASS TRANSFER EFFECTS ON UNSTEADY HYDROMAGNETIC CONVECTIVE FLOW PAST A VERTICAL POROUS PLATE IN A POROUS MEDIUM WITH HEAT SOURCE

G. NARSIMLU^{1,*}, T. SUDHAKAR RAO²

¹Chaitanya Bharathi Institute of Technology, Hyderabad, India

²Vasavi college of engineering, Hyderabad, India

Copyright © 2021 the author(s). This is an open access article distributed under the Creative Commons Attribution License, which permits unrestricted use, distribution, and reproduction in any medium, provided the original work is properly cited.

Abstract: The objective of this chapter is to analyze the effect of mass transfer on unsteady hydromagnetic free convective flow of a viscous incompressible electrically conducting fluid past an infinite vertical porous plate in presence of constant suction and heat source. The governing equations of the flow field are solved using Galerkin finite element method and approximate solutions are obtained for velocity field, temperature field, concentration distribution, skin friction and the rate of heat and mass transfer. The numerical results for some special cases were compared with Das *et al.* [7] and were found to be in good agreement. The effects of the flow parameters such as Hartmann number (M), Grashof number for heat and mass transfer (Gr , Gc), Permeability parameter (Kp), Schmidt number (Sc), Heat source parameter (S), Prandtl number (Pr) and Eckert number (Ec) on the flow field are analyzed with the help of figures. The problem has some relevance in the geophysical and astrophysical studies.

Keywords: hydromagnetic; mass transfer; free convection; porous medium; suction; heat source; Galerkin finite element method.

2010 AMS Subject Classification: 80A20.

*Corresponding author

E-mail address: gnr.cbit@gmail.com

Received May 23, 2021

1. INTRODUCTION

The phenomenon of hydromagnetic flow with heat and mass transfer in an electrically conducting fluid past a porous plate embedded in a porous medium has attracted the attention of a good number of investigators because of its varied applications in many engineering problems such as MHD generators, plasma studies, nuclear reactors, oil exploration, geothermal energy extractions and in the boundary layer control in the field of aerodynamics. Heat transfer in laminar flow is important in problems dealing with chemical reactions and in dissociating fluids.

In view of its wide applications, Hasimoto [8] initiated the boundary layer growth on a flat plate with suction or injection. Soundalgekar [17] showed the effect of free convection on steady MHD flow of an electrically conducting fluid past a vertical plate. Yamamoto and Iwamura [18] explained the flow of a viscous fluid with convective acceleration through a porous medium. Mansutti *et al.* [12] have discussed the steady flow of a non-Newtonian fluid past a porous plate with suction or injection. Jha [9] analyzed the effect of applied magnetic field on transient free convective flow in a vertical channel.

Chandran *et al.*, [2] have discussed the unsteady free convection flow of an electrically conducting fluid with heat flux and accelerated boundary layer motion in presence of a transverse magnetic field. Acharya *et al.* [1] have reported the problem of heat and mass transfer over an accelerating surface with heat source in presence of suction and blowing. The unsteady free convective MHD flow with heat transfer past a semi-infinite vertical porous moving plate with variable suction has been studied by Kim [10]. Singh and Thakur [16] have given an exact solution of a plane unsteady MHD flow of a non-Newtonian fluid. Sharma and Pareek [14] explained the behaviour of steady free convective MHD flow past a vertical porous moving surface. Singh *et al.*, [15] have analyzed the effect of heat and mass transfer in MHD flow of a viscous fluid past a vertical plate under oscillatory suction velocity. Makinde *et al.* [11] discussed the unsteady free convective flow with suction on an accelerating porous plate. Sarangi and Jose [13] studied the unsteady free convective MHD flow and mass transfer past a vertical porous plate with variable temperature. Das *et al.*, [3] estimated the mass transfer effects on unsteady flow past an accelerated vertical porous plate with suction employing finite difference analysis. Das *et al.* [4] investigated numerically the unsteady free convective MHD flow past an accelerated vertical plate with suction and heat flux. Das and Mitra [5] discussed the unsteady

mixed convective MHD flow and mass transfer past an accelerated infinite vertical plate with suction.

Recently, Das *et al.* [6] analyzed the effect of mass transfer on MHD flow and heat transfer past a vertical porous plate through a porous medium under oscillatory suction and heat source. More recently, Das *et al.* [7] investigated the hydromagnetic convective flow past a vertical porous plate through a porous medium with suction and heat source. The study of stellar structure on solar surface is connected with mass transfer phenomena. Its origin is attributed to difference in temperature caused by the non - homogeneous production of heat which in many cases can rest not only in the formation of convective currents but also in violent explosions. Mass transfer certainly occurs within the mantle and cores of planets of the size of or larger than the earth. In the present study we therefore, propose to analyze the effect of mass transfer on unsteady free convective flow of a viscous incompressible electrically conducting fluid past an infinite vertical porous plate with constant suction and heat source in presence of a transverse magnetic field. This paper basically highlights the effect of mass transfer on hydromagnetic flow in presence of suction and heat source.

2. MATHEMATICAL FORMULATION

Consider the unsteady free convective mass transfer flow of a viscous incompressible electrically conducting fluid past an infinite vertical porous plate in presence of constant suction and heat source and transverse magnetic field. Let the x' - axis be taken in vertically upward direction along the plate and y' - axis normal to it. The physical sketch and geometry of the problem is shown in figure A. Within the above framework, the equations which govern the flow under the usual Boussinesq's approximation are as follows

Continuity Equation:

$$\frac{\partial v'}{\partial y'} = 0 \Rightarrow v' = -v_o' \text{ (Constant)} \quad (1)$$

Momentum Equation:

$$\frac{\partial u'}{\partial t'} + v' \frac{\partial u'}{\partial y'} = g\beta(T' - T_\infty') + g\beta^*(C' - C_\infty') + v \frac{\partial^2 u'}{\partial y'^2} - \frac{\sigma B_o^2}{\rho} u' - \frac{v}{K} u' \quad (2)$$

Energy Equation:

$$\frac{\partial T'}{\partial t'} + v' \frac{\partial T'}{\partial y'} = K \frac{\partial^2 T'}{\partial y'^2} + \frac{v}{C_p} \left(\frac{\partial u'}{\partial y'} \right)^2 + S'(T' - T_\infty) \quad (3)$$

Concentration Equation:

$$\frac{\partial C'}{\partial t'} + v' \frac{\partial C'}{\partial y'} = D \frac{\partial^2 C'}{\partial y'^2} \quad (4)$$

The boundary conditions of the problem are:

$$\left. \begin{aligned} u' = 0, v' = -v_o', T' = T_w' + \varepsilon(T_w' - T_\infty') e^{i\omega t'}, C' = C_w' + \varepsilon(C_w' - C_\infty') e^{i\omega t'} \text{ at } y' = 0 \\ u' \rightarrow 0, T' \rightarrow T_\infty', C' \rightarrow C_\infty' \text{ as } y' \rightarrow \infty \end{aligned} \right\} \quad (5)$$

Introducing the following non-dimensional variables and parameters,

$$\left. \begin{aligned} y = \frac{y' v_o'}{v}, t = \frac{t' v_o'^2}{4v}, \omega = \frac{4v\omega'}{v_o'^2}, u = \frac{u'}{v_o'}, v = \frac{\eta_o}{\rho}, M = \left(\frac{\sigma B_o'^2}{\rho} \right) \frac{v}{v_o'^2}, K_p = \frac{v_o'^2 K'}{v^2}, \\ \theta = \frac{T' - T_\infty'}{T_w' - T_\infty'}, C = \frac{C' - C_\infty'}{C_w' - C_\infty'}, Pr = \frac{v}{k}, Gr = \frac{vg\beta(T_w' - T_\infty')}{v_o'^3}, Gc = \frac{vg\beta^*(C_w' - C_\infty')}{v_o'^3}, \\ Sc = \frac{v}{D}, S = \frac{4S'v}{v_o'^2}, Ec = \frac{v_o'^2}{C_p(T_w' - T_\infty')} \end{aligned} \right\} \quad (6)$$

where $g, \rho, \sigma, v, \beta, \beta^*, \omega, \eta_o, k, \theta, T_w', T_\infty', C, C_w', C_\infty', C_p, D, Pr, Sc, Gr, Gc, S, K_p, Ec$ and M are respectively the acceleration due to gravity, density, electrical conductivity, coefficient of kinematic viscosity, volumetric coefficient of expansion for heat transfer, volumetric coefficient of expansion for mass transfer, angular frequency, coefficient of viscosity, thermal diffusivity, temperature, temperature at the plate, temperature at infinity, concentration, concentration at the plate, concentration at infinity, specific heat at constant pressure, molecular mass diffusivity, Prandtl number, Schmidt number, Grashof number for heat transfer, Grashof number for mass transfer, heat source parameter, permeability parameter, Eckert number and Hartmann number.

Substituting (6) in equations (2), (3) and (4) under boundary conditions (5), we get:

$$\frac{1}{4} \frac{\partial u}{\partial t} - \frac{\partial u}{\partial y} = (Gr)\theta + (Gc)C + \frac{\partial^2 u}{\partial y^2} - \left(M + \frac{1}{K_p} \right) u \quad (7)$$

$$\frac{1}{4} \frac{\partial \theta}{\partial t} - \frac{\partial \theta}{\partial y} = \frac{1}{Pr} \frac{\partial^2 \theta}{\partial y^2} + \frac{1}{4} S\theta + (Ec) \left(\frac{\partial u}{\partial y} \right)^2 \quad (8)$$

$$\frac{1}{4} \frac{\partial C}{\partial t} - \frac{\partial C}{\partial y} = \frac{1}{Sc} \frac{\partial^2 C}{\partial y^2} \quad (9)$$

The corresponding boundary conditions are:

$$\left. \begin{aligned} u = 0, \theta = 1 + \varepsilon e^{i\omega t}, C = 1 + \varepsilon e^{i\omega t} \quad \text{at } y = 0 \\ u \rightarrow 0, \theta \rightarrow 0, C \rightarrow 0 \quad \text{as } y \rightarrow \infty \end{aligned} \right\} \quad (10)$$

3. METHOD OF SOLUTION

By applying Galerkin finite element method for equation (7) over the element (e), ($y_j \leq y \leq y_k$)

is:

$$\int_{y_j}^{y_k} \left\{ N^T \left[4 \frac{\partial^2 u^{(e)}}{\partial y^2} - \frac{\partial u^{(e)}}{\partial t} + 4 \frac{\partial u^{(e)}}{\partial y} - 4Au^{(e)} + P \right] \right\} dy = 0 \quad (11)$$

Where $A = M + \frac{1}{Kp}$, $P = 4(Gr)\theta + 4(Gc)C$;

Integrating the first term in equation (11) by parts one obtains

$$N^{(e)T} \left\{ 4 \frac{\partial u^{(e)}}{\partial y} \right\}_{y_j}^{y_k} - \int_{y_j}^{y_k} \left\{ 4 \frac{\partial N^{(e)T}}{\partial y} \frac{\partial u^{(e)}}{\partial y} + N^{(e)T} \left(\frac{\partial u^{(e)}}{\partial t} - 4 \frac{\partial u^{(e)}}{\partial y} + 4Au^{(e)} - P \right) \right\} dy = 0 \quad (12)$$

Neglecting the first term in equation (12), one gets:

$$\int_{y_j}^{y_k} \left\{ 4 \frac{\partial N^{(e)T}}{\partial y} \frac{\partial u^{(e)}}{\partial y} + N^{(e)T} \left(\frac{\partial u^{(e)}}{\partial t} - 4 \frac{\partial u^{(e)}}{\partial y} + 4Au^{(e)} - P \right) \right\} dy = 0$$

Let $u^{(e)} = N^{(e)}\phi^{(e)}$ be the linear piecewise approximation solution over the element (e)

($y_j \leq y \leq y_k$), where $N^{(e)} = [N_j \quad N_k]$, $\phi^{(e)} = [u_j \quad u_k]^T$ and $N_j = \frac{y_k - y}{y_k - y_j}$, $N_k = \frac{y - y_j}{y_k - y_j}$ are

the basis functions. One obtains:

$$\int_{y_j}^{y_k} \left\{ 4 \begin{bmatrix} N'_j & N'_j & N'_j & N'_k \\ N'_j & N'_k & N'_k & N'_k \end{bmatrix} \begin{bmatrix} u_j \\ u_k \end{bmatrix} \right\} dy + \int_{y_j}^{y_k} \left\{ \begin{bmatrix} N_j & N_j & N_j & N_k \\ N_j & N_k & N_k & N_k \end{bmatrix} \begin{bmatrix} \dot{u}_j \\ \dot{u}_k \end{bmatrix} \right\} dy - 4 \int_{y_j}^{y_k} \left\{ \begin{bmatrix} N_j & N'_j & N_j & N'_k \\ N'_j & N_k & N'_k & N_k \end{bmatrix} \begin{bmatrix} u_j \\ u_k \end{bmatrix} \right\} dy \\ + 4A \int_{y_j}^{y_k} \left\{ \begin{bmatrix} N_j & N_j & N_j & N_k \\ N_j & N_k & N_k & N_k \end{bmatrix} \begin{bmatrix} u_j \\ u_k \end{bmatrix} \right\} dy = P \int_{y_j}^{y_k} \begin{bmatrix} N_j \\ N_k \end{bmatrix} dy$$

Simplifying we get

$$\frac{4}{l^{(e)^2}} \begin{bmatrix} 1 & -1 \\ -1 & 1 \end{bmatrix} \begin{bmatrix} u_j \\ u_k \end{bmatrix} + \frac{1}{6} \begin{bmatrix} 2 & 1 \\ 1 & 2 \end{bmatrix} \begin{bmatrix} \dot{u}_j \\ \dot{u}_k \end{bmatrix} - \frac{4}{2l^{(e)}} \begin{bmatrix} -1 & 1 \\ -1 & 1 \end{bmatrix} \begin{bmatrix} u_j \\ u_k \end{bmatrix} + \frac{4A}{6} \begin{bmatrix} 2 & 1 \\ 1 & 2 \end{bmatrix} \begin{bmatrix} u_j \\ u_k \end{bmatrix} = \frac{P}{2} \begin{bmatrix} 1 \\ 1 \end{bmatrix}$$

Where prime and dot denotes differentiation w.r.t 'y' and time 't' respectively. Assembling the element equations for two consecutive elements $y_{i-1} \leq y \leq y_i$ and $y_i \leq y \leq y_{i+1}$ following is obtained:

$$\frac{4}{l^{(e)^2}} \begin{bmatrix} 1 & -1 & 0 \\ -1 & 2 & -1 \\ 0 & -1 & 1 \end{bmatrix} \begin{bmatrix} u_{i-1} \\ u_i \\ u_{i+1} \end{bmatrix} + \frac{1}{6} \begin{bmatrix} 2 & 1 & 0 \\ 1 & 4 & 1 \\ 0 & 1 & 2 \end{bmatrix} \begin{bmatrix} \dot{u}_{i-1} \\ \dot{u}_i \\ \dot{u}_{i+1} \end{bmatrix} - \frac{4}{2l^{(e)}} \begin{bmatrix} -1 & 1 & 0 \\ -1 & 0 & 1 \\ 0 & -1 & 1 \end{bmatrix} \begin{bmatrix} u_{i-1} \\ u_i \\ u_{i+1} \end{bmatrix} \\ + \frac{4A}{6} \begin{bmatrix} 2 & 1 & 0 \\ 1 & 4 & 1 \\ 0 & 1 & 2 \end{bmatrix} \begin{bmatrix} u_{i-1} \\ u_i \\ u_{i+1} \end{bmatrix} = \frac{P}{2} \begin{bmatrix} 1 \\ 2 \\ 1 \end{bmatrix} \quad (13)$$

Now put row corresponding to the node 'i' to zero, from equation (13) the difference schemes with $l^{(e)} = h$ is:

$$\frac{4}{h^2} [-u_{i-1} + 2u_i - u_{i+1}] + \frac{1}{6} \begin{bmatrix} \dot{u}_{i-1} + 4\dot{u}_i + \dot{u}_{i+1} \end{bmatrix} - \frac{4}{2h} [-u_{i-1} + u_{i+1}] + \frac{4A}{6} [u_{i-1} + 4u_i + u_{i+1}] = P \quad (14)$$

Applying the trapezoidal rule, following system of equations in Crank-Nicholson method are obtained:

$$A_1 u_{i-1}^{n+1} + A_2 u_i^{n+1} + A_3 u_{i+1}^{n+1} = A_4 u_{i-1}^n + A_5 u_i^n + A_6 u_{i+1}^n + 12Pk \quad (15)$$

Now from equations (8) and (9), following equations are obtained:

$$G_1\theta_{i-1}^{n+1} + G_2\theta_i^{n+1} + G_3\theta_{i+1}^{n+1} = G_4\theta_{i-1}^n + G_5\theta_i^n + G_6\theta_{i+1}^n + 12Qk \quad (16)$$

$$J_1C_{i-1}^{n+1} + J_2C_i^{n+1} + J_3C_{i+1}^{n+1} = J_4C_{i-1}^n + J_5C_i^n + J_6C_{i+1}^n \quad (17)$$

Where $A_1 = 2 + 4Ak + 12rk - 24r$; $A_2 = 16Ak + 48r + 8$; $A_3 = 2 + 4Ak - 12rh - 24r$;

$$A_4 = 2 - 4Ak - 12rh + 24r; A_5 = 8 - 16Ak - 48r; A_6 = 2 - 4Ak + 12rh + 24r;$$

$$G_1 = 2(Pr) + 12rh(Pr) - S(Pr)k - 24r; G_2 = 8(Pr) + 48r - 4S(Pr)k;$$

$$G_3 = 2(Pr) - 12rh(Pr) - 24r - S(Pr)k; G_4 = 2(Pr) - 12rh(Pr) + 24r + S(Pr)k;$$

$$G_5 = 8(Pr) - 48r + 4S(Pr)k; G_6 = 2(Pr) + 12rh(Pr) + 24r + S(Pr)k;$$

$$J_1 = 2(Sc) + 12rh(Sc) - 24r; J_2 = 8(Sc) + 48r; J_3 = 2(Sc) - 12rh(Sc) - 24r;$$

$$J_4 = 2(Sc) - 12rh(Sc) + 24r; J_5 = 8(Sc) - 48r; J_6 = 2(Sc) + 12rh(Sc) + 24r;;$$

$$P = 4(Gr)\theta_i^j + 4(Gc)C_i^j; Q = 4(Pr)(Ec)k \left(\frac{\partial u_i^j}{\partial y} \right)^2$$

Here $r = \frac{k}{h^2}$ and h, k are mesh sizes along y - direction and time - direction respectively. Index

'i' refers to space and 'j' refers to the time. In the equations (15), (16) and (17) taking $i = 1(1) n$ and using boundary conditions (10), then the following system of equations are obtained:

$$A_i X_i = B_i \quad i = 1(1)3 \quad (18)$$

Where A_i 's are matrices of order n and X_i, B_i 's are column matrices having n-components. The solutions of above system of equations are obtained by using Thomas algorithm for velocity, temperature and concentration. Also, numerical solutions for these equations are obtained by C - programme. In order to prove the convergence and stability of Galerkin finite element method, the same C - programme was run with smaller values of h and k and no significant change was observed in the values of u, θ and C. Hence the Galerkin finite element method is stable and convergent.

Shear Stress and Rate of Heat and Mass Transfer:

The skin friction at the plate in the direction of velocity is given by

$$\tau = \left(\frac{\partial u}{\partial y} \right)_{y=0}$$

Heat transfer coefficient (Nu) at the plate is $Nu = - \left(\frac{\partial \theta}{\partial y} \right)_{y=0}$

Mass transfer coefficient (Sh) at the plate is $Sh = - \left(\frac{\partial C}{\partial y} \right)_{y=0}$

4. RESULTS AND DISCUSSION

The effect of mass transfer on unsteady free convective flow of a viscous incompressible electrically conducting fluid past an infinite vertical porous plate with constant suction and heat source in presence of a transverse magnetic field has been studied. The governing equations of the flow field are solved by applying Galerkin finite element method and approximate solutions are obtained for velocity field, temperature field, concentration distribution, skin friction and rate of heat and mass transfer. The effects of the pertinent parameters on the flow field are analyzed and discussed with the help of velocity profiles (figures 1 - 5), temperature profiles (figures 6 - 8) and concentration distribution (figure 9). To be more realistic, during numerical calculations we have chosen the values of $Pr = 0.71$ representing air at $20^\circ C$, $Sc = 0.60$ representing H_2O vapour, $Gr > 0$ corresponding to cooling of the plate and $S > 0$ representing heat source.

Velocity field:

The velocity of the flow field is found to change more or less with the variation of the flow six parameters. The major factors affecting the velocity of the flow field are Hartmann number M , Permeability parameter Kp , Grashof number for heat and mass transfer (Gr , Gc); and Heat source parameter S . The effects of these parameters on the velocity field have been analyzed with the help of figures 1 - 5.

The effect of the Hartmann number (M) is shown in figure (1). It is observed that the velocity of the fluid decreases with the increase of the magnetic field number values. The decrease in the velocity as the Hartmann number (M) increases is because the presence of a magnetic field in an electrically conducting fluid introduces a force called the Lorentz force, which acts against the flow if the magnetic field is applied in the normal direction, as in the present study. This resistive force slows down the fluid velocity component as shown in figure (1). Figure (2) shows the effect of the permeability of the porous medium parameter Kp on the velocity distribution. As shown, the velocity is increasing with the increasing dimensionless porous medium parameter. The effect of the dimensionless porous medium Kp becomes smaller as Kp increase. Physically, this result can be achieved when the holes of the porous medium may be neglected.

The temperature and the species concentration are coupled to the velocity via Grashof number Gr and Modified Grashof number Gc as seen in equation (7). For various values of Grashof number and Modified Grashof number, the velocity profiles 'u' are plotted in figures (3) and (4). The Grashof number Gr signifies the relative effect of the thermal buoyancy force to the viscous hydrodynamic force in the boundary layer. As expected, it is observed that there is a rise in the velocity due to the enhancement of thermal buoyancy force. Also, as Gr increases, the peak values of the velocity increases rapidly near the porous plate and then decays smoothly to the free stream velocity. The Modified Grashof number (Gc) defines the ratio of the species buoyancy force to the viscous hydrodynamic force. As expected, the fluid velocity increases and the peak value is more distinctive due to increase in the species buoyancy force. The velocity distribution attains a distinctive maximum value in the vicinity of the plate and then decreases properly to approach the free stream value. It is noticed that the velocity increases with increasing values of the Modified Grashof number.

Figure (5) shows the collective effects of heat source parameter S for conducting air ($Pr = 0.71$) in the case of cooling plate ($Gr > 0$), i.e., the free convection currents convey heat away from the plate into the boundary layer. With an increase in S from 0.0 to 0.9, there is a clear increase in the velocity, i.e., the flow is accelerated. When heat is generated, the buoyancy force increases, which accelerates the flow rate and thereby giving, rise to the increase in the velocity profiles. These velocity profiles are closely agreed with existed results of Das *et al.* [7].

Temperature field:

The temperature of the flow field suffers a substantial change with the variation of the flow parameters such as Prandtl number Pr , Eckert number Ec and Heat source parameter S . These variations are shown in figures (6) – (8). The temperature profiles are in good agreement with those of Das *et al.* [7]. In figure (6) we depict the effect of Prandtl number (Pr) on the temperature field. It is observed that an increase in the Prandtl number leads to decrease in the temperature field. Also, temperature field falls more rapidly for water in comparison to air and the temperature curve is exactly linear for mercury, which is more sensible towards change in temperature. From this observation it is conclude that mercury is most effective for maintaining temperature differences and can be used efficiently in the laboratory. Air can replace mercury, the effectiveness of maintaining temperature changes are much less than mercury. However, air can be better and cheap replacement for industrial purpose. This is because, either increase of kinematic viscosity or decrease of thermal conductivity leads to increase in the value of Prandtl number (Pr). Hence temperature decreases with increasing of Prandtl number (Pr).

The temperature profiles θ are depicted in figures (7) and (8) for different values of Eckert number Ec and Heat source parameter S . The fluid temperature attains its maximum value at the plate surface, and decreases gradually to free stream zero value far away from the plate. It is seen that the fluid temperature increases with a rise in Ec . In the present study, we restrict our attention to the positive values of Ec , which corresponds to plate cooling, i.e., loss of heat from the plate to the fluid. Also, we note that increasing Ec causes an increase in Joule heating as the magnetic field adds energy to the fluid boundary layer due to the work done in dragging the fluid. Therefore, the fluid temperature is noticeably enhanced with an increase in S from 0.0 to 0.9. This increase in the temperature profiles is accompanied by the simultaneous increase in the thermal boundary layer thickness.

Concentration distribution:

The effect of Schmidt number (Sc) on the concentration field is presented in figure (9). Figure (9) shows the concentration field due to variation in Schmidt number (Sc) for the gasses Hydrogen, Helium, Water-vapour, Oxygen and Ammonia. It is observed that concentration field is steadily for Hydrogen and falls rapidly for Oxygen and Ammonia in comparison to Water-vapour. Thus Hydrogen can be used for maintaining effective concentration field and Water-vapour can be used for maintaining normal concentration field.

Skin friction:

The values of skin friction at the wall against Kp for different values of Hartmann number M and heat source parameter S are shown in the figures (10) and (11) respectively. From figure (10), it is observed that a growing Hartmann number M reduces the skin friction at the wall for a fixed value of the permeability parameter due to the action of Lorentz force in the flow field. It is further observed from figure (11) that heat source parameter S enhance the skin friction at the wall. Our observation for skin friction agrees with those of Das *et al.* [7].

Rate of heat and mass transfer:

The rate of heat transfer at the wall varies with the variation of Hartmann number M , Heat source parameter S against Prandtl number Pr are shown in the figures (12) and (13). From figure (12), we observe that a growing heat source parameter increases the magnitude of the rate of heat transfer at the wall. Further, it is observed that from figure (13) that an increase in Hartmann number reduces its value for a given value of Prandtl number due to the magnetic pull of the Lorentz force acting on the flow field. These variations agree with those of Das *et al.* [7] with a little deviation for all the values of M . The rate of mass transfer at the wall varies with the variation of Schmidt number Sc against y is shown in the figure (14). From figure (14), we observe that a growing Schmidt number decreases the magnitude of the rate of heat transfer at the wall. In order to ascertain the accuracy of the numerical results, the present results are compared with the existed results of Das *et al.*, [7] for different values of M in the figure (15). They are found to be in a good agreement.

5. CONCLUSIONS

We summarize below the following results of physical interest on the velocity, temperature and the concentration distribution of the flow field and also on the wall shear stress and rate of heat transfer at the wall.

1. A growing Hartmann number retards the velocity of the flow field at all points.
2. The effect of increasing Grashof number for heat and mass transfer or heat source parameter is to accelerate velocity of the flow field at all points.
3. The velocity of the flow field increases with an increase in permeability parameter and heat source parameter.

4. A growing Eckert number or heat source parameter increases temperature of the flow field at all points.
5. The Prandtl number Pr increases the temperature of the flow field at all points
6. The effect of increasing Schmidt number is to reduce the concentration boundary layer thickness of the flow field at all points.
7. A growing Hartmann number reduces the skin friction at the wall while a growing heat source parameter reverses the effect against the permeability parameter.
8. The effect of increasing heat source parameter is to increase the magnitude of the rate of heat transfer at the wall. On the other hand, a growing Hartmann number reduces its value for a given value of Prandtl number due to the magnetic pull of the Lorentz force acting on the flow field.
9. The effect of increasing Schmidt number is to decrease the magnitude of the rate of mass transfer at the wall.
10. In order to ascertain the accuracy of the numerical results, the present results are compared with the existed results of Das *et al.*, [7] for velocity, temperature, concentration, skin friction, rate of heat and mass transfer. They are found to be in a good agreement.

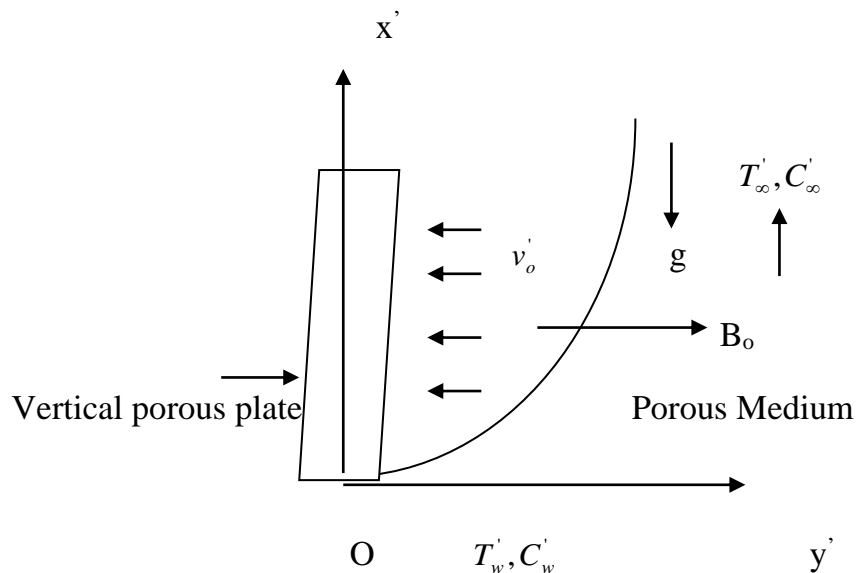


Figure A. Physical sketch and geometry of the problem

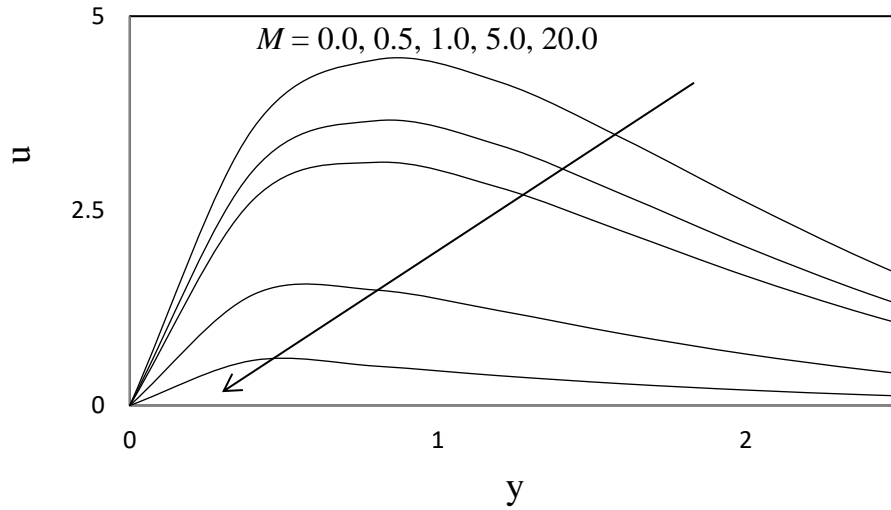


Figure 1. Velocity profiles against y for different values of M with $Gr = 5.0$, $Gc = 5.0$, $Pr = 0.71$, $Sc = 0.60$, $Kp = 1.0$, $S = 0.1$, $Ec = 0.002$, $\varepsilon = 0.2$, $\omega = 1.0$ and $\omega t = \pi/2$.

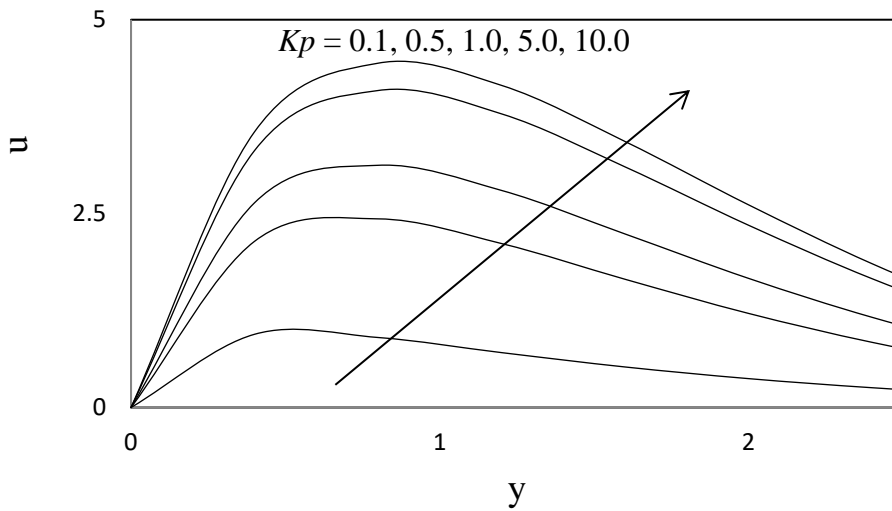


Figure 2. Velocity profiles against y for different values of Kp with $Gr = 5.0$, $Gc = 5.0$, $Pr = 0.71$, $Sc = 0.60$, $M = 1.0$, $S = 0.1$, $Ec = 0.002$, $\varepsilon = 0.2$, $\omega = 1.0$ and $\omega t = \pi/2$.

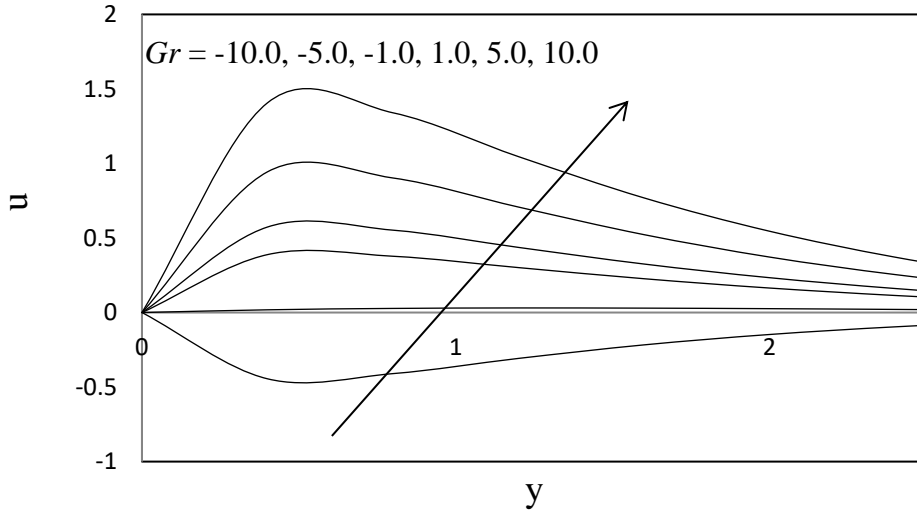


Figure 3. Velocity profiles against y for different values of Gr with $Gc = 5.0$, $Kp = 1.0$, $Pr = 0.71$, $Sc = 0.60$, $M = 1.0$, $S = 0.1$, $Ec = 0.002$, $\varepsilon = 0.2$, $\omega = 1.0$ and $\omega t = \pi/2$.

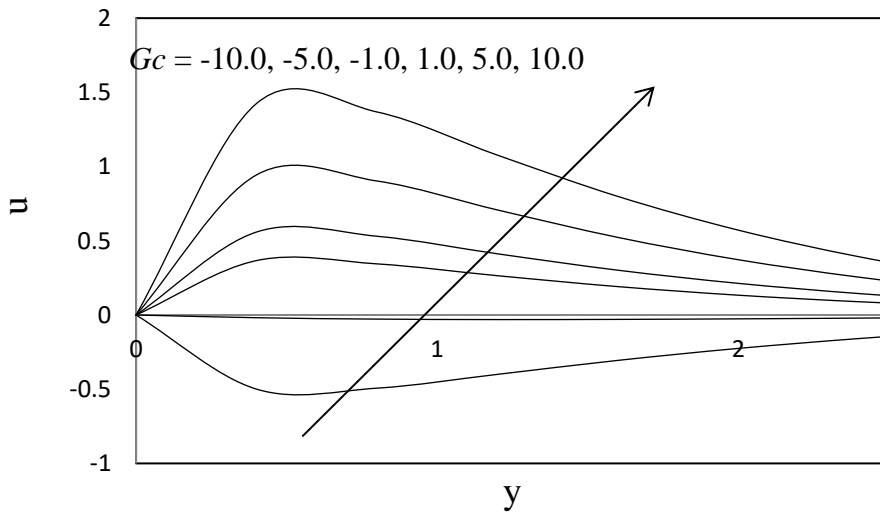


Figure 4. Velocity profiles against y for different values of Gc with $Gr = 5.0$, $Kp = 1.0$, $Pr = 0.71$, $Sc = 0.60$, $M = 1.0$, $S = 0.1$, $Ec = 0.002$, $\varepsilon = 0.2$, $\omega = 1.0$ and $\omega t = \pi/2$.

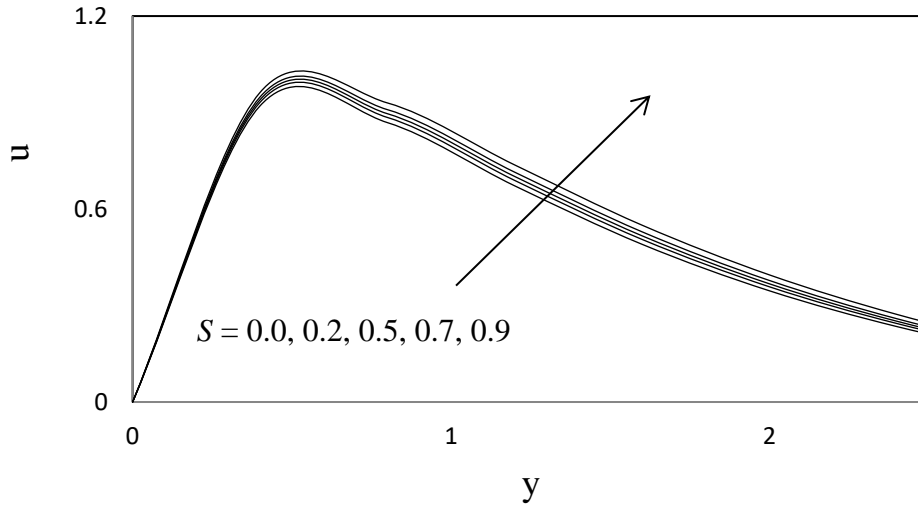


Figure 5. Velocity profiles against y for different values of S with $Gr = 5.0$, $Gr = 5.0$, $Kp = 1.0$, $Pr = 0.71$, $Sc = 0.60$, $M = 1.0$, $Ec = 0.002$, $\varepsilon = 0.2$, $\omega = 1.0$ and $\omega t = \pi/2$.

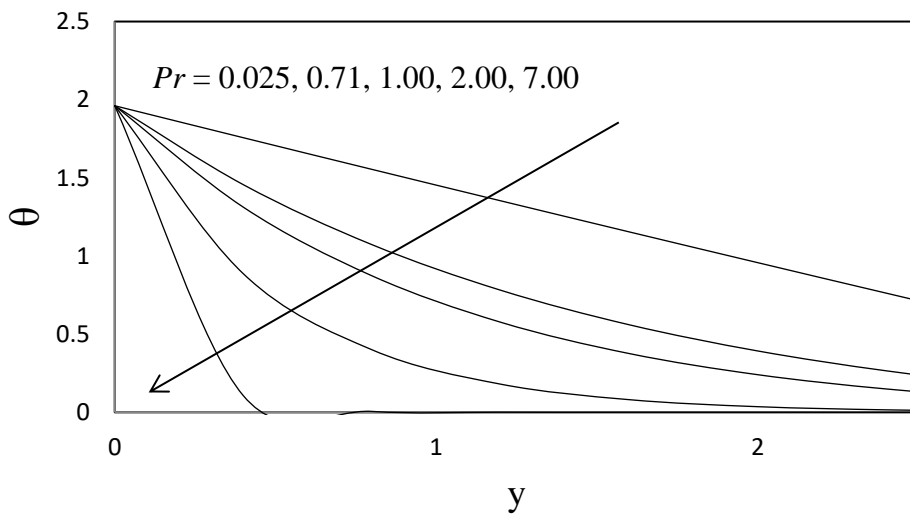


Figure 6. Temperature profiles against y for different values of Pr with $Gr = 5.0$, $Gr = 5.0$, $Kp = 1.0$, $Sc = 0.60$, $Ec = 0.002$, $M = 1.0$, $S = 0.1$, $\varepsilon = 0.2$, $\omega = 1.0$ and $\omega t = \pi/2$.

FINITE ELEMENT SOLUTION OF MASS TRANSFER EFFECTS

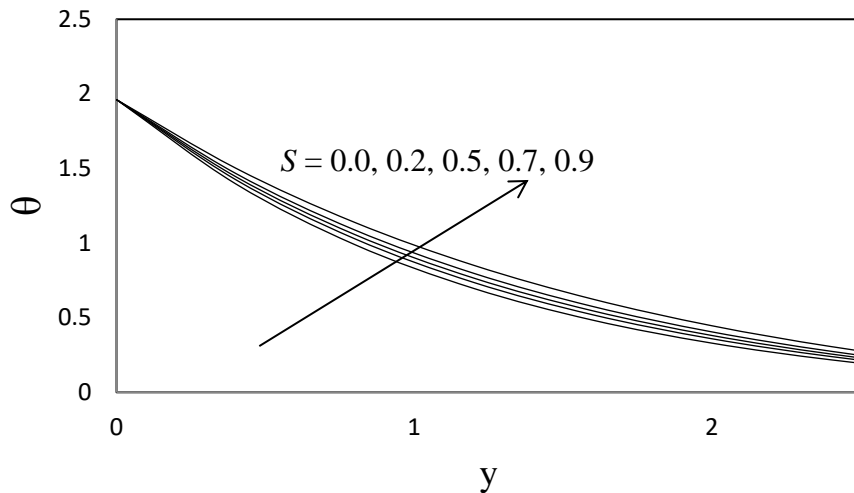


Figure 7. Temperature profiles against y for different values of S with $Gr = 5.0$, $Gr = 5.0$, $Kp = 1.0$, $Pr = 0.71$, $Sc = 0.60$, $M = 1.0$, $Ec = 0.002$, $\varepsilon = 0.2$, $\omega = 1.0$ and $\omega t = \pi/2$.

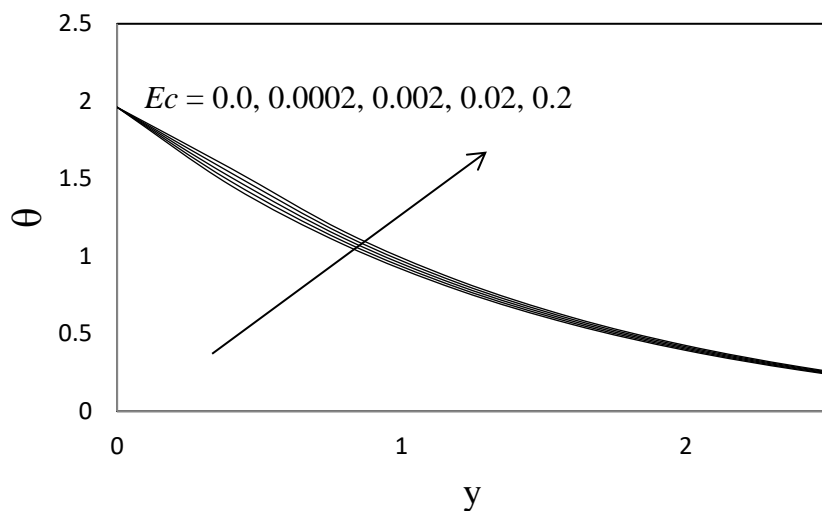


Figure 8. Temperature profiles against y for different values of Ec with $Gr = 5.0$, $Gr = 5.0$, $Kp = 1.0$, $Pr = 0.71$, $Sc = 0.60$, $M = 1.0$, $S = 0.1$, $\varepsilon = 0.2$, $\omega = 1.0$ and $\omega t = \pi/2$.

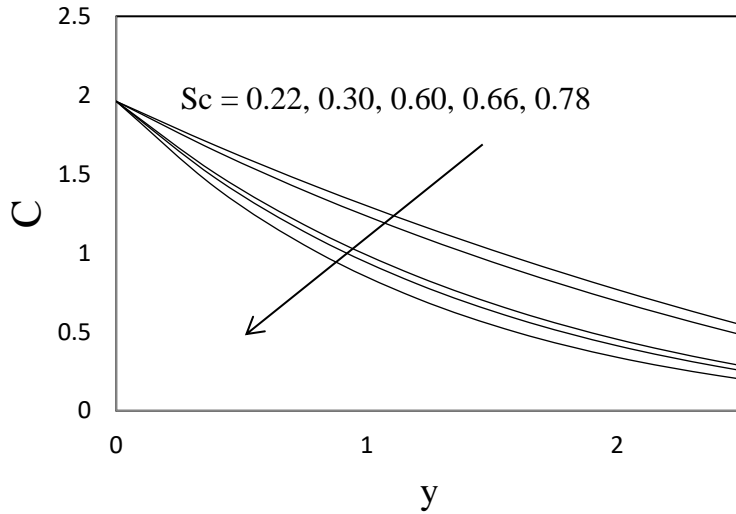


Figure 9. Concentration profiles against y for different values of Sc with $Gr = 5.0$, $Gr = 5.0$, $Kp = 1.0$, $Pr = 0.71$, $Ec = 0.002$, $M = 1.0$, $S = 0.1$, $\varepsilon = 0.2$, $\omega = 1.0$ and $\omega t = \pi/2$.

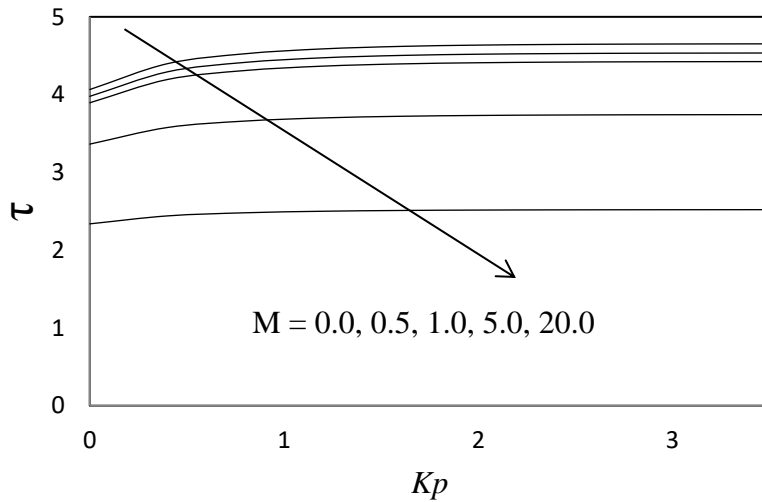


Figure 10. Skin friction profiles against Kp for different values of M with $Gr = 5.0$, $Gr = 5.0$, $Pr = 0.71$, $Sc = 0.60$, $S = 0.1$, $Ec = 0.002$, $\varepsilon = 0.2$, $\omega = 1.0$ and $\omega t = \pi/2$.

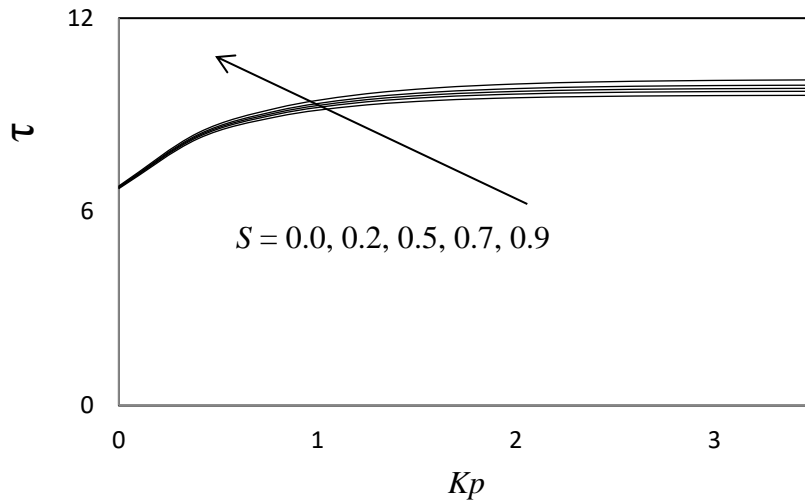


Figure 11. Skin friction profiles against Kp for different values of S with $Gr = 5.0$, $Gr = 5.0$, $Pr = 0.71$, $Sc = 0.60$, $M = 1.0$, $Ec = 0.002$, $\varepsilon = 0.2$, $\omega = 1.0$ and $\omega t = \pi/2$.

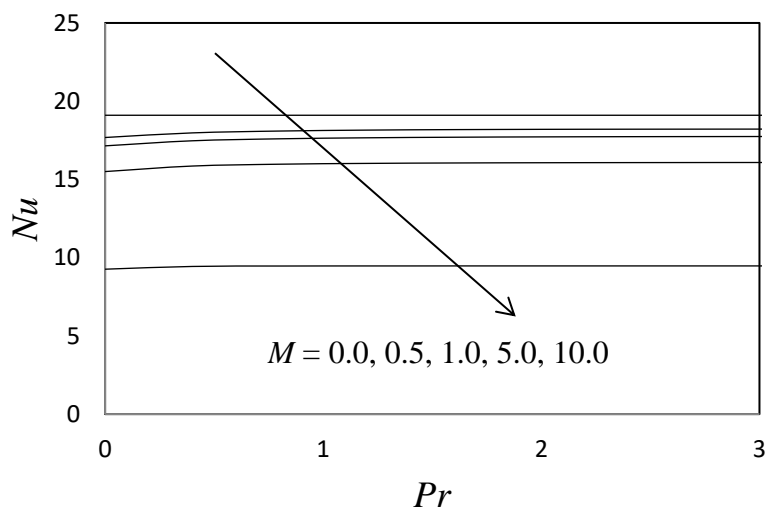


Figure 12. Rate of heat transfer (Nu) against Pr for different values of M with $Gr = 5.0$, $Gr = 5.0$, $Kp = 1.0$, $Sc = 0.60$, $S = 0.1$, $Ec = 0.002$, $\varepsilon = 0.2$, $\omega = 1.0$ and $\omega t = \pi/2$.

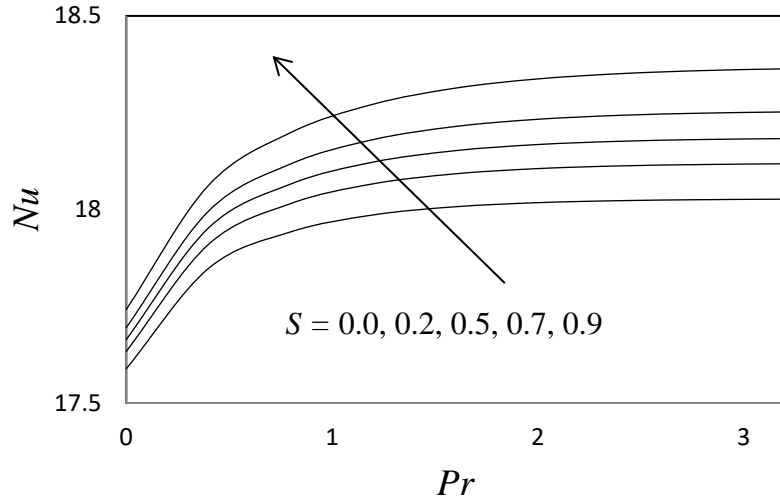


Figure 13. Rate of heat transfer (Nu) against Pr for different values of S with $Gr = 5.0$, $Gr = 5.0$, $Kp = 1.0$, $Sc = 0.60$, $M = 1.0$, $Ec = 0.002$, $\varepsilon = 0.2$, $\omega = 1.0$ and $\omega t = \pi/2$.

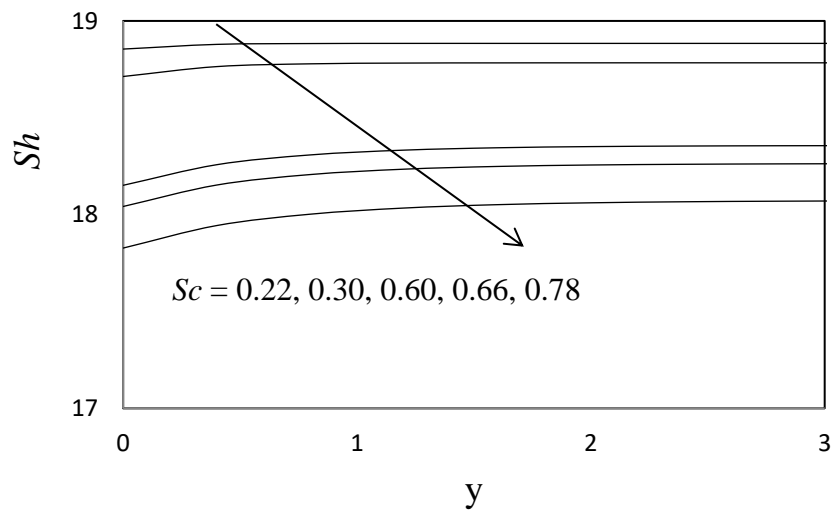


Figure 14. Rate of mass transfer (Sh) against y for different values of Sc with $Gr = 5.0$, $Gr = 5.0$, $Kp = 1.0$, $S = 0.1$, $M = 1.0$, $Ec = 0.002$, $\varepsilon = 0.2$, $\omega = 1.0$ and $\omega t = \pi/2$.

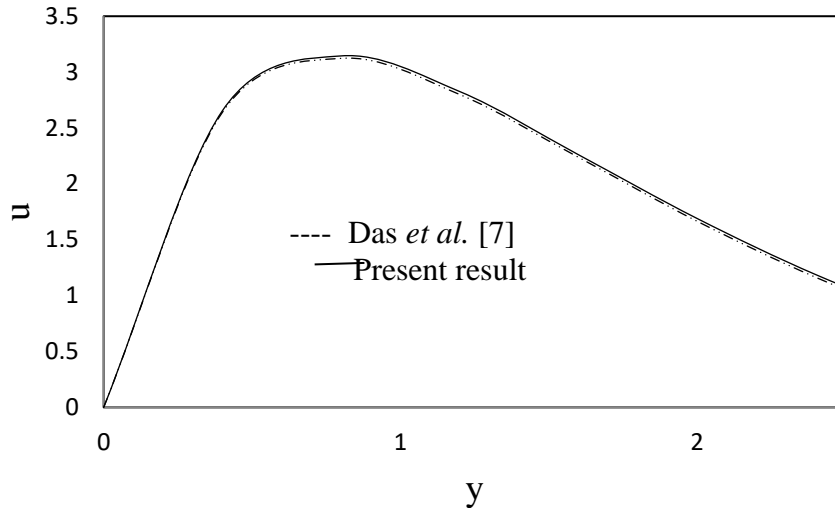


Figure 15. Velocity profiles against y for different values of M with $Gr = 5.0$, $Gc = 5.0$, $Pr = 0.71$, $Sc = 0.60$, $Kp = 1.0$, $S = 0.1$, $Ec = 0.002$, $\varepsilon = 0.2$, $\omega = 1.0$ and $\omega t = \pi/2$.

CONFLICT OF INTERESTS

The author(s) declare that there is no conflict of interests.

REFERENCES

- [1] M. Acharya, L. P. Singh, G. C. Dash, Heat and mass transfer over an accelerating surface with heat source in presence of suction and blowing, *Int. J. Eng. Sci.* 37 (1999) 189–211.
- [2] P. Chandran, N. C. Sacheti, A. K. Singh, Unsteady hydromagnetic free convection flow with heat flux and accelerated boundary motion. *J. Phys. Soc. Japan* 67 (1998) 124-129.
- [3] S. S. Das, S. K. Sahoo, G. C. Dash, Numerical solution of mass transfer effects on unsteady flow past an accelerated vertical porous plate with suction. *Bull. Malays. Math. Sci. Soc.* 29 (2006), 33-42.
- [4] S. S. Das, A. Satapathy, J. K. Das, S. K. Sahoo, Numerical solution of unsteady free convective MHD flow past an accelerated vertical plate with suction and heat flux, *J. Ultra Sci. Phys. Sci.* 19 (2007), 105-112.
- [5] S. S. Das, M. Mitra, Unsteady mixed convective MHD flow and mass transfer past an accelerated infinite vertical plate with suction, *Indian J. Sci. Technol.* 2 (2009), 18-22.
- [6] S. S. Das, A. Satapathy, J. K. Das, J. P. Panda, Mass transfer effects on MHD flow and heat transfer past a vertical porous plate through a porous medium under oscillatory suction and heat source. *Int. J. Heat Mass Transfer* 52 (2009), 5962-5969.
- [7] S. S. Das, U. K. Tripathy, J. K. Das, Hydromagnetic convective flow past a vertical porous plate through a porous medium with suction and heat source, *Int. J. Energy Environ.* 1 (2010), 467-478.

- [8] H. Hasimoto, Boundary layer growth on a flat plate with suction or injection, *J. Phys. Soc. Japan* 12 (1957), 68-72.
- [9] B. K. Jha, Effects of applied magnetic field on transient free convective flow in a vertical channel. *Indian J. Pure Appl. Math.* 29 (1998), 441-445.
- [10] Y. J. Kim, Unsteady MHD convective heat transfer past a semi-infinite vertical porous moving plate with variable suction. *Int. J. Eng. Sci.* 38 (2000), 833-845.
- [11] O. D. Makinde, J. M. Mango, D. M. Theuri, Unsteady free convection flow with suction on an accelerating porous plate. *AMSE J. Mod. Meas. Cont.* 72 (2003), 39-46.
- [12] D. Mansutti, G. Pontrelli, K. R. Rajagopal, Steady flows of non-Newtonian fluids past a porous plate with suction or injection. *Int. J. Num. Meth. Fluids* 17 (1993), 927-941.
- [13] K. C. Sarangi, C. B. Jose, Unsteady free convective MHD flow and mass transfer past a vertical porous plate with variable temperature. *Bull. Cal. Math. Soc.* 97 (2005), 137-146.
- [14] P. R. Sharma, D. Pareek, Steady free convection MHD flow past a vertical porous moving surface, *Indian J. Theor. Phys.* 50 (2002), 5-13.
- [15] A. K. Singh, A. K. Singh, N. P. Singh, Heat and mass transfer in MHD flow of a viscous fluid past a vertical plate under oscillatory suction velocity, *Indian J. Pure Appl. Math.* 34 (2003), 429-442.
- [16] B. Singh, C. Thakur, An exact solution of plane unsteady MHD non-Newtonian fluid flows. *Indian J. Pure Appl. Math.* 33 (2002), 993 -1001.
- [17] V. M. Soundalgekar, Free convection effects on steady MHD flow past a vertical porous plate, *J. Fluid Mech.* 66 (1974), 541-551.
- [18] K. Yamamoto, N. Iwamura, Flow with convective acceleration through a porous medium. *Eng. Math.* 10 (1976), 41-54.